

ROCK signaling is involved in the entosis of both nonepithelial and epithelial tumors, whereas N-cadherin is involved in the entosis of nonepithelial tumors

MIZUHA OI, RAIK KUSHIBIKI, YUKI KANEHIRA, YOSHIMI NISHIJIMA,
SAYAKA KOBAYASHI and MASANAO SAIO

Laboratory of Histopathology and Cytopathology, Department of Laboratory Sciences,
Gunma University Graduate School of Health Sciences, Maebashi, Gunma 371-8514, Japan

Received December 13, 2024; Accepted February 13, 2025

DOI: 10.3892/etm.2025.12840

Abstract. Entosis is a cell-in-cell phenomenon wherein cells detaching from the extracellular matrix are internalized by a neighboring cell. The present study examined whether entosis, which is observed in epithelial cells, also occurs in nonepithelial cells. The present study used the MCF-7 breast cancer cell line as a positive control for entosis and compared this with three representative sarcoma cell lines (RD, HT1080 and ICH-ERMS-1). The formation of cell-in-cell structures was induced by culturing cells in adherent and nonadherent conditions. Cell lines that formed the cell-in-cell structures were cultured in nonadherent conditions with and without Rho-associated coiled-coil containing protein kinase (ROCK) inhibition, and the cell-in-cell structures were evaluated in slides prepared from cell blocks. It was examined whether ROCK inhibition blocked the formation of cell-in-cell structures, and the expression levels of specific cadherins associated with entosis were determined using quantitative PCR. The proportion of cells with cell-in-cell structures was significantly higher in nonadherent conditions in both MCF-7 ($P=0.0297$) and RD ($P=0.0098$) cells, whereas few cell-in-cell structures were observed in both adherent and nonadherent conditions in HT1080 and ICH-ERMS-1 cells. Under nonadherent conditions, ROCK inhibition significantly reduced the proportion of cells with cell-in-cell structures in MCF-7 ($P=0.0021$) and RD ($P=0.0407$) cells. Based on quantitative PCR, among the five cadherin genes, the E-cadherin expression level was the lowest in MCF-7 cells (ΔCt , 2.6) and the N-cadherin expression level was lowest in RD cells (ΔCt , 4.8).

By contrast, the N-cadherin expression levels were higher in HT1080 (ΔCt , 11.0) and ICH-ERMS-1 (ΔCt , 8.8) cells. These results suggested that the cell-in-cell phenomenon observed in RD cells is an entotic process based on its emergence in nonadherent culture conditions and the involvement of ROCK signaling. Entosis observed in RD cells was mediated via N-cadherin and not E-cadherin.

Introduction

Cell-in-cell (CIC) structures result from the internalization of one or more living cells by a neighboring cell, where the internalized cells are surrounded by a large vacuole (1,2). The inner and outer cells can be of the same type (homotypic CIC) or different types (heterotypic CIC) (3). CIC structures have been observed in various cancers, including breast (4,5), lung (6,7), tongue (8), gastric (9), and pancreatic cancers (10) and melanoma (11) as well as in cytologically malignant samples from urine and effusion fluids (12). CIC structures are associated with several cellular processes, including cannibalism, emperipolesis, and entosis (2,13). In tumor cells, cannibalism refers to the phagocytic engulfment of other tumor or immune cells by a tumor cell to acquire nutrients or escape from the immune system (11,14). Emperipolesis, derived from the Greek meaning 'inside around wandering about,' describes the penetration and residence of inflammatory cells within host cells, such as tumor cells and megakaryocytes, without being destroyed (15,16). Entosis, derived from the Greek word 'entos,' meaning inside/into/within, was first described by Overholtzer *et al* (1) as the internalization of one cell by a neighboring cell, triggered by the detachment of the cell from the extracellular matrix.

Although the recent recognition of entosis as a concept, studies utilizing the human mammary epithelial cell line MCF-10A and the breast cancer cell line MCF-7 cells (1,17) reveal that epithelial cadherin (E-cadherin), placental cadherin (P-cadherin) (17) and α -catenin (3) as well as the Rho/Rho-associated coiled-coil containing protein kinase (ROCK)/actomyosin signaling in internalized cells play crucial roles in entosis. During this process, neighboring cells compete with each other and one cell becomes the host cell,

Correspondence to: Professor Masanao Saio, Laboratory of Histopathology and Cytopathology, Department of Laboratory Sciences, Gunma University Graduate School of Health Sciences, 39-22, 3-chome, Showa-machi, Maebashi, Gunma 371-8514, Japan
E-mail: saio@gunma-u.ac.jp

Key words: entosis, cell-in-cell structures, rhabdomyosarcoma, Rho-associated coiled-coil containing protein kinase, N-cadherin

the outer cell whereas the other cell becomes the internalized cell (18), Sun *et al* (18) demonstrated that cells expressing E-cadherin and higher levels of phospho-myosin light chain 2 were more likely to become internalized cells both in MCF-10A and MCF-7 cells and that MCF-10A cells harboring mutant *KRAS* exhibited a deformable cell membrane mediated via Rac1 signaling, rendering them to become host cells. The internalized cells may undergo lysosomal cell death in MCF-7 cells (1) and may proceed to mitosis, escape, or survival within the host cell in the breast cancer cell line MDA-MB-453 (18). The role of entosis in cancer remains unclear, with conflicting findings and different perspectives (19). Entosis can lead to the generation of aneuploid cells, as the presence of the inner cell physically inhibits the cytokinesis of the host cell, resulting in binucleated host cells in models utilizing MCF10A and MCF-7 cells (20). Conversely, entosis related to p53 can contribute to the elimination of aneuploid cells resulting from prolonged mitosis in MCF10A and MCF-7 cells (21).

Clinical studies have also reported the association of entosis with cancer outcomes. Dziuba *et al* (5) found that the frequency of entosis was associated with a high Ki-67 index and lymph node metastasis in patients with HER2-positive mammary breast cancer. Additionally, Wen *et al* (22) reported that the rate of entotic structures was higher in patients with castration-resistant human prostate cancer than in those with benign prostate hyperplasia or androgen-dependent prostate cancer. The same study also revealed that androgen receptor increased the frequency of entosis by inhibiting phosphoinositide 3-kinase and the RhoA/ROCK signaling in LNCaP cells, a prostate cancer cell line (22). Furthermore, entosis has been linked to both favorable and poor prognoses in certain cancers. For example, homotypic CIC in cancer cells was an indicator of favorable outcomes in patients with breast cancer (23) whereas entosis was more prevalent in patients with unfavorable prognosis in pancreatic ductal adenocarcinoma (10).

Despite considerable advances made in understanding the underlying entosis (17), it is still primarily considered a phenomenon observed in epithelial cells (1), with evidence coming from a variety of sources, including mammary epithelial (24), breast cancer (25), bronchial epithelial (26), lung cancer (27), pancreatic carcinoma (10), colon cancer (26,28), and epidermoid carcinoma (27,29) cell lines. To date, no studies have explored whether entosis might also occur in nonepithelial cells. Therefore, the aim of this study was to investigate whether entosis can occur in nonepithelial cells under nonadherent conditions which typically support entosis in epithelial cells.

Materials and methods

Samples. The following cell lines were purchased from the JCRB Cell Bank managed by the National Institutes of Biomedical Innovation, Health, and Nutrition (Osaka, Japan): MCF-7 breast cancer cells (JCRB0134), RD rhabdomyosarcoma cells (JCRB9072), HT1080 fibrosarcoma cells (IFO50354), and ICH-ERMS-1 rhabdomyosarcoma cells (JCRB1648). All cell lines were confirmed to be negative for mycoplasma by the JCRB Cell Bank.

Cell culture. All cell lines were cultured in Dulbecco's modified Eagle's medium (DMEM; 043-30085; FujiFilm Wako

Pure Chemical, Osaka, Japan) supplemented with 10% fetal bovine serum (S1600-500, Biowest, Nuaille, France) and 1% penicillin-streptomycin (168-23191; FujiFilm Wako Pure Chemical) at 37°C in a humidified 5% CO₂ atmosphere.

Cell internalization assay. Cell internalization was evaluated in cultures maintained in 24-well cell plates for adherent (3473; Corning, NY, USA) and nonadherent (174930; Thermo Fisher Scientific Inc, Massachusetts, USA) cultures. First, the cells were cultured in 75-cm² cell culture flasks (130190; Thermo Fisher Scientific Inc.) to a density of 1.0-2.0x10⁵ cells/ml, detached using 0.25% Trypsin-ethylenediaminetetraacetic acid (EDTA) (Trypsin; 27250018; FUJIFILM Wako Pure Chemical Corporation, EDTA; E5134; SIGMA, Massachusetts, USA), and adjusted to a density of 0.8-1.0x10⁵ cells/ml. Next, 1 ml of the prepared cell suspensions was added to each well of the adherent and nonadherent plates, which were then incubated for 6 h. In adherent plates, following medium removal from six wells, the wells were rinsed with 1 ml phosphate-buffered saline (PBS; FUJIFILM Wako Pure Chemical Corporation), 120 µl of 0.25% Trypsin-EDTA was added to each well of the plate, which was incubated for 5 min at 37°C. To terminate the reaction, 1 ml fresh DMEM was added to each well, and all cells were collected into one tube and centrifuged at 180 x g for 5 min at room temperature. The supernatant was discarded, and the cell pellet was transferred to a 1.5-ml microtube for cell block preparation. In nonadherent plates, trypsinization was performed after the collection of cells from the plates, as they were not adherent to the plate. Briefly, for each treatment condition, cells from six wells were collected in a centrifuge tube, which was centrifuged at 180 x g for 5 min at room temperature. The supernatants were discarded, and the cells were resuspended in 10 ml PBS. After centrifugation at 180 x g for 5 min at room temperature, the supernatant was discarded, 1 ml of 0.25% Trypsin-EDTA was added to each tube, and the resuspended cells were incubated for 5 min at 37°C. Next, 4 ml fresh DMEM was added to each tube to terminate the reaction, followed by centrifugation and the transfer of the cell pellets to 1.5-ml microtubes for cell block preparation.

Cell internalization assay with the ROCK inhibitor treatment in nonadherent cultures. A 20-mM stock solution of the ROCK inhibitor Y27632 (CS-0131; ChemScene, NJ, USA) was prepared by dissolving 5 mg of Y27632 in 1 ml of dimethyl sulfoxide (DMSO; D2650; Sigma Aldrich, Milwaukee, WI, USA). The working solutions for the ROCK inhibitor and DMSO were prepared by adding 25 µl of the stock solution to 25 ml of DMEM, followed by sterilization with filtration. For treatment with the ROCK inhibitor, 0.5 ml of the cell suspension at a density of 1.6-2.0x10⁵ cells/ml was added to each well, followed by the addition of 0.5 ml of DMEM containing 20 µM Y27632 or DMSO. Next, the cell internalization assay for nonadherent cultures was performed as described above.

Cell block preparation. Approximately 30 µl of a 2% fibrinogen solution (F3879; Sigma Aldrich) in PBS (FujiFilm Wako Pure Chemical) was added to the cell pellets in microtubes, and finger tapping was used for gentle mixing. Immediately after adding 20 µl of the thrombin solution (224092751;

Table I. Primers used for PCR in the present study.

Primer	Forward (5'-3')	Reverse (5'-3')	Tm (°C)
E-cadherin	aggaggagattttgagcacgt	ttgggttgggtcgttgact	59.8
M-cadherin	gtcatctacagcatccaggg	aggaaggctggccggttgct	60.0
N-cadherin	ggcagaagagagactgggctc	gaggctggtcagctcctggc	60.0
P-cadherin	aacctccacagccaccatag	aaactgctcctcctcacggt	60.0
R-cadherin	ccgaccagcccccattggag	cctggcttg gagcctcgtcc	60.0
GAPDH	aggtgaaggtcggagtcaac	gcctcgcctccttctgattt	60.0

Tm, melting temperature.

Mochida Pharmaceutical, Tokyo, Japan), the microtubes were gently tapped to mix the solution and incubated for 5 min for clotting. The fibrin clot was collected using forceps, placed into an embedding cassette (USM-1900-W; Youken Science, Tokyo, Japan), and fixed overnight in 10% neutral buffered formalin solution (062-01661; FujiFilm Wako Pure Chemical).

Embedding and sectioning of cell blocks. After fixation, the specimens were processed using a vacuum infiltration processor (Tissue-Tek VIP; Sakura Finetek Japan, Tokyo, Japan) and embedded in paraffin. Four- μ m-thick sections were prepared using a rotary microtome (RX-860; Yamato Kohki Industrial, Saitama, Japan) attached to a continuous cooling device (PC-110; Yamato Kohki Industrial) to ensure cooling during slicing.

Hematoxylin and hematoxylin/eosin staining. The slides prepared from cell blocks were soaked in xylene (242-00087; FujiFilm Wako Pure Chemical) three times, 5 min each, followed by 100, 95, and 70% ethanol, for 1 min each. The slides were rinsed under running water for 1 min, followed by staining with Mayer's hematoxylin (30141; New Hematoxylin Type M; Muto Pure Chemicals, Tokyo, Japan) for 10 min. Following rinsing under running water for 10 min, the slides were stained with eosin (32081; New Eosin Type M; Muto Pure Chemicals) for 3 min. After a brief rinse under running water, the slides were dipped in 70 and 95% ethanol, five times each. The slides were dipped in 100% ethanol twice, for 30 sec each, and in xylene three times, for 5 min each. Finally, the slides were sealed using a mounting medium (20093; Malinol; Muto Pure Chemicals) and observed under a microscope (Olympus BX51; Olympus Corporation, Tokyo, Japan). For hematoxylin-only staining, the slides were processed as described above, except for immersion in eosin.

Evaluation of the CIC structures. The hematoxylin/eosin-stained slides were evaluated to observe the CIC structures, and images of the CIC structures in the entire viewing area were captured using a digital microscope with an affixed camera (DP23; Olympus Corporation) using a 100x oil-immersion objective lens. The capture settings were as follows: exposure, auto; gain, 2x; exposure compensation, 2/3; and resolution, 2072x2072 pixels. Each cell exhibiting the morphological characteristics of engulfing more than two-thirds of another cell was counted as one CIC structure.

CIC structures were assessed by one cytotechnologist and one pathologist, and consensus between the two observers was recorded.

Whole-slide imaging. Whole-slide imaging of the slides stained with hematoxylin/eosin or hematoxylin alone were captured using a digital slide scanner (Nano Zoomer-SQ C13140-01; Hamamatsu Photonics, Shizuoka, Japan). The scanning settings were as follows: objective lens, 20x; numerical aperture, 0.75; scanning speed, 40x; maximum capture size, 26x76 mm²; pixel size, 0.23 μ m/pixel; diode source, light-emitting; image storage format, JPEG; and focus, automatic.

Cell counting by computer-assisted image analysis. Whole-slide images of hematoxylin-stained slides were converted to MRXS files using an image converter software (version 1.14) from 3DHISTECH (Budapest, Hungary). The files were analyzed to count cell nuclei using the HistoQuant module in the Panoramic Viewer software (3DHISTECH). The HistoQuant settings were as follows: hue, 252-310; saturation: 25-53; separation, 7; noise reduction (Gauss), 3; minimum size, 23; and maximum size, 211. Of note, these settings were slightly adjusted depending on the staining condition for precise identification of the cellular nuclei in each sample (Table SI).

Quantitative polymerase chain reaction (qPCR). Total RNA extraction was performed using TRIzolTM reagent (15596-026; Thermo Fisher Scientific) according to the manufacturer's instructions. The synthesis of cDNA was performed using SuperScriptTM III Reverse Transcriptase (18080-044; Thermo Fisher Scientific) according to the manufacturer's instructions. Candidate genes were measured using qPCR system according to the manufacturer's protocol of PowerUpTM SYBRTM Green master mix (A25742; Thermo Fisher Scientific) described. The reaction conditions were as follows for primer pairs with a melting temperature (Tm) at or above 60°C: 1 cycle at 50°C for 2 min and 95°C for 2 min, followed by 40 cycles at 95°C for 15 sec and 60°C for 1 min. For primer pairs with a Tm below 60°C, the reaction conditions were as follows: 1 cycle at 50°C for 2 min and 95°C for 2 min, followed by 40 cycles at 95°C for 15 sec, Tm of the primer-pair (Table I) for 15 sec, and 72°C for 1 min. In all reactions, melting curve analysis was performed for reaction specificity, and the single melting curve gained reaction was considered specific. The primers

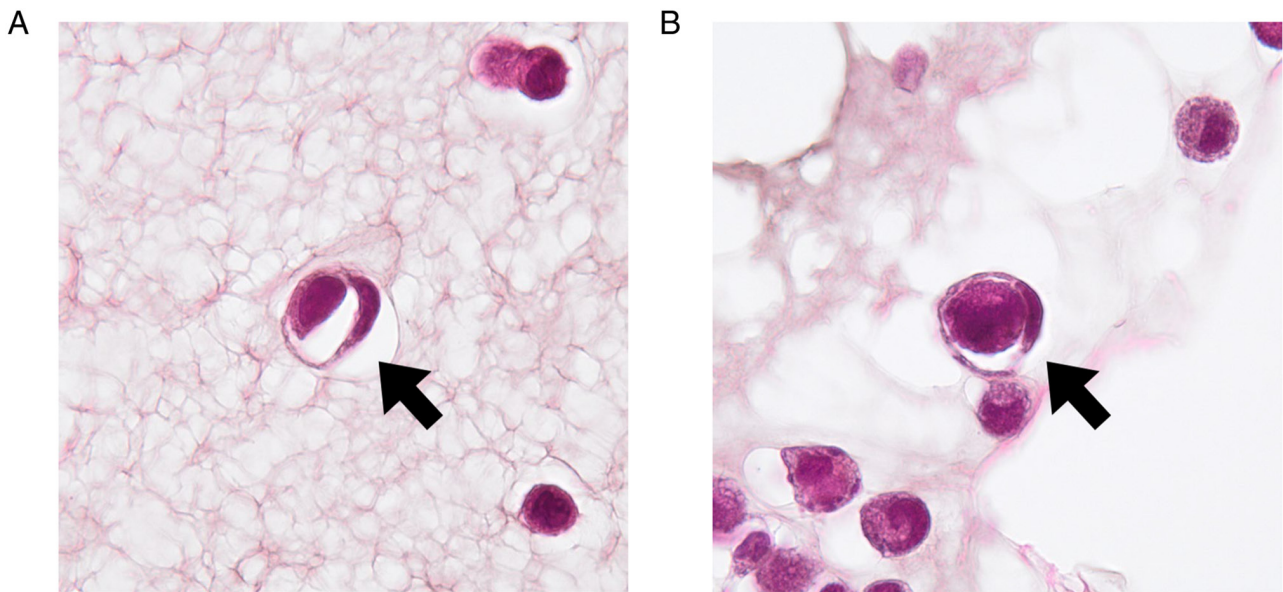


Figure 1. Representative images of CIC structures in cultures of (A) MCF-7 and (B) RD cells stained with hematoxylin and eosin. Magnification, x100. Black arrows indicate the CIC phenomenon. CIC, cell-in-cell.

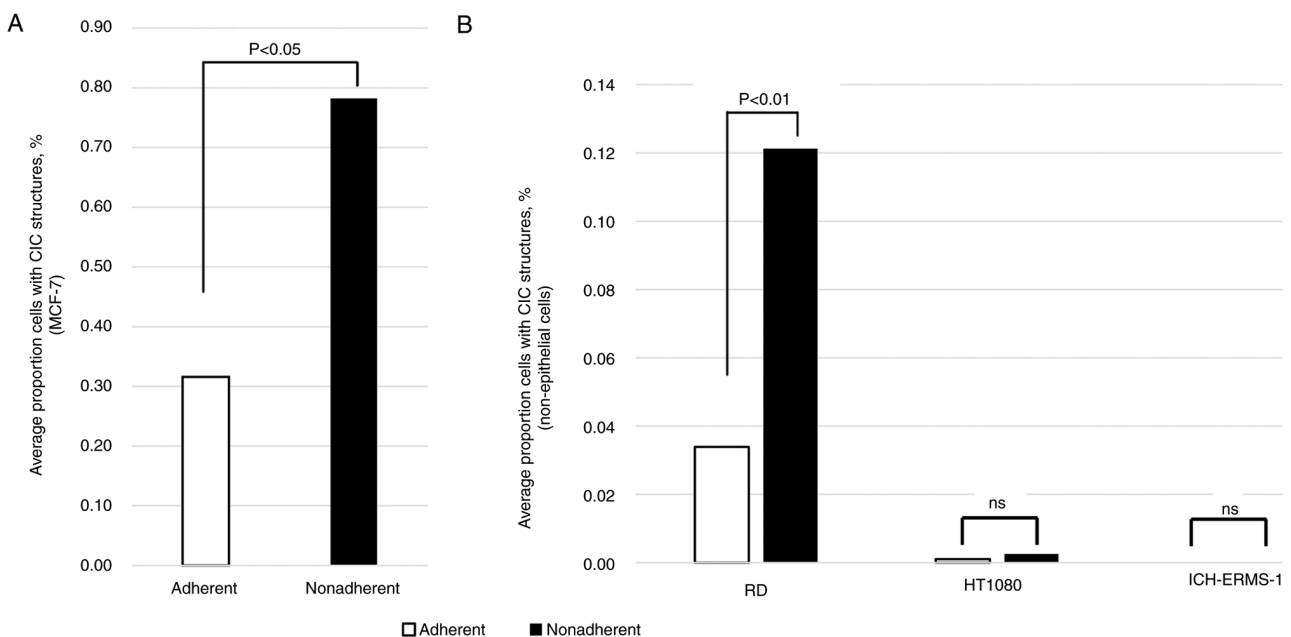


Figure 2. Comparison of the proportion of cells with CIC structures in (A) MCF-7 cells and (B) sarcoma cell lines cultured in adherent and nonadherent conditions. CIC, cell-in-cell; ns, not significant.

used for qPCR were synthesized at FASMAC (Kanagawa, Japan) and purchased from Greiner Bio-One (Tokyo, Japan) (Table I). Delta Ct (Δ Ct) value was calculated based on the following formula: Δ Ct = Ct (a target gene) - Ct (a reference gene: GAPDH) (30).

Statistical analysis. All data were analyzed using JMP Pro version 15 (SAS Institute, Tokyo, Japan). For the analysis of the cell internalization assay, Welch's t-test was used to compare means and the Wilcoxon rank-sum test was used for nonparametric comparisons between two groups. A P value of <0.05 was considered to indicate statistical significance.

Results

CIC structures are observed in rhabdomyosarcoma cell lines under nonadherent conditions. Although widely documented in epithelial cells under nonadherent conditions (1), whether entosis can occur in nonepithelial cells remains unknown. Therefore, we determined whether rhabdomyosarcoma cells exhibited entosis under nonadherent culture conditions. To this end, we compared the proportion of cells with CIC structures in a range of cell lines grown in adherent and nonadherent tissue culture plates. A representative CIC structure is shown in Fig. 1. As shown in Fig. 2A and B, the proportion of cells

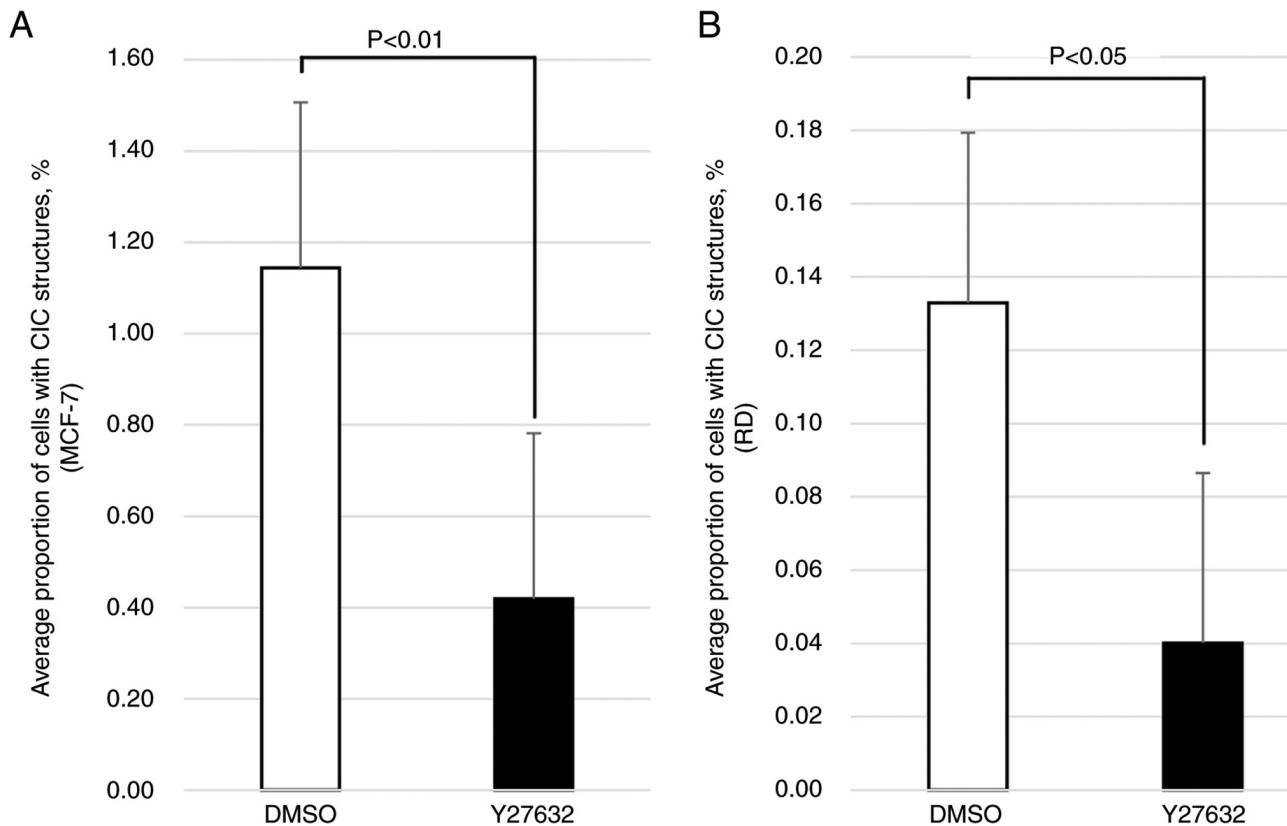


Figure 3. Effect of Rho-associated coiled-coil containing protein kinase inhibition with Y27632 on the proportion of cells with CIC structures in (A) MCF-7 and (B) RD cells. DMSO was used as the vehicle for Y27632. CIC, cell-in-cell.

with CIC structures was significantly higher in nonadherent culture conditions than in adherent culture conditions in both the MCF-7 and RD cell lines ($P=0.0297$ and $P=0.0098$ respectively). However, the proportion of cells with CIC structures was low in adherent conditions and did not significantly change in nonadherent conditions in either the HT1080 or ICH-ERMS-1 cell lines. These results suggested that CIC structures could emerge not only in epithelial but also in nonepithelial cells.

Inhibition of ROCK signaling blocks the emergence of CIC structures in rhabdomyosarcoma cells. Previous studies (17,18) demonstrated that entosis could be blocked by the inhibition of ROCK with Y27632 (31). To determine whether the CIC structures observed in the RD cell line represented entosis, we evaluated the proportion of cells with CIC structures in RD and MCF-7 cells cultured in nonadherent conditions and treated with Y27632. As shown in Fig. 3, the proportion of cells with CIC structures was significantly decreased in both the MCF-7 ($P=0.0021$) and RD ($P=0.0407$) cells treated with Y27632 compared with the cultures treated with the DMSO vehicle, suggesting that the emergence of CIC structures observed in the RD cells cultured in nonadherent conditions was due to entosis, which was also observed in the MCF-7 cells, the positive control.

N-cadherin is involved in entosis in rhabdomyosarcoma cells. To investigate the molecular mechanisms underlying entosis in rhabdomyosarcoma cells, we compared the expression levels of the members of the cadherin family of genes

using quantitative PCR between the entotic MCF-7 and RD cell lines and the nonentotic HT1080 and ICH-ERMS-1 cell lines. As shown in Fig. 4, the E-cadherin expression level was the lowest among the five cadherin genes in the MCF-7 cell line, with a ΔCt value of 2.6. Conversely, the neural cadherin (N-cadherin) expression level was lowest among the five cadherin genes in the RD cell line, with a ΔCt value of 4.8. However, the N-cadherin expression levels were relatively higher in the HT1080 (ΔCt value of 11.0) and ICH-ERMS-1 (ΔCt value of 8.8) cell lines compared with the RD cell line (Fig. 4). Overall, these results suggested that E-cadherin and N-cadherin were involved in entosis in the MCF-7 and RD cell lines, respectively.

Discussion

The sequential activation of RhoA, ROCK, and phospho-myosin light chain 2 leads to the contraction of actomyosin, resulting in entosis (32); indeed, ROCK inhibition was shown to block entosis (17,18). In the present study, we found that the CIC structures observed in the nonepithelial rhabdomyosarcoma cell line RD were triggered by the detachment of cells from the matrix in nonadherent culture conditions and that these structures were blocked by ROCK inhibition, thereby demonstrating that entosis could occur not only in epithelial but also in nonepithelial cell lines. In addition, we found that the core adhesion molecule involved in the entosis of nonepithelial cells was N-cadherin and not E-cadherin, which was previously shown to be involved in epithelial cell

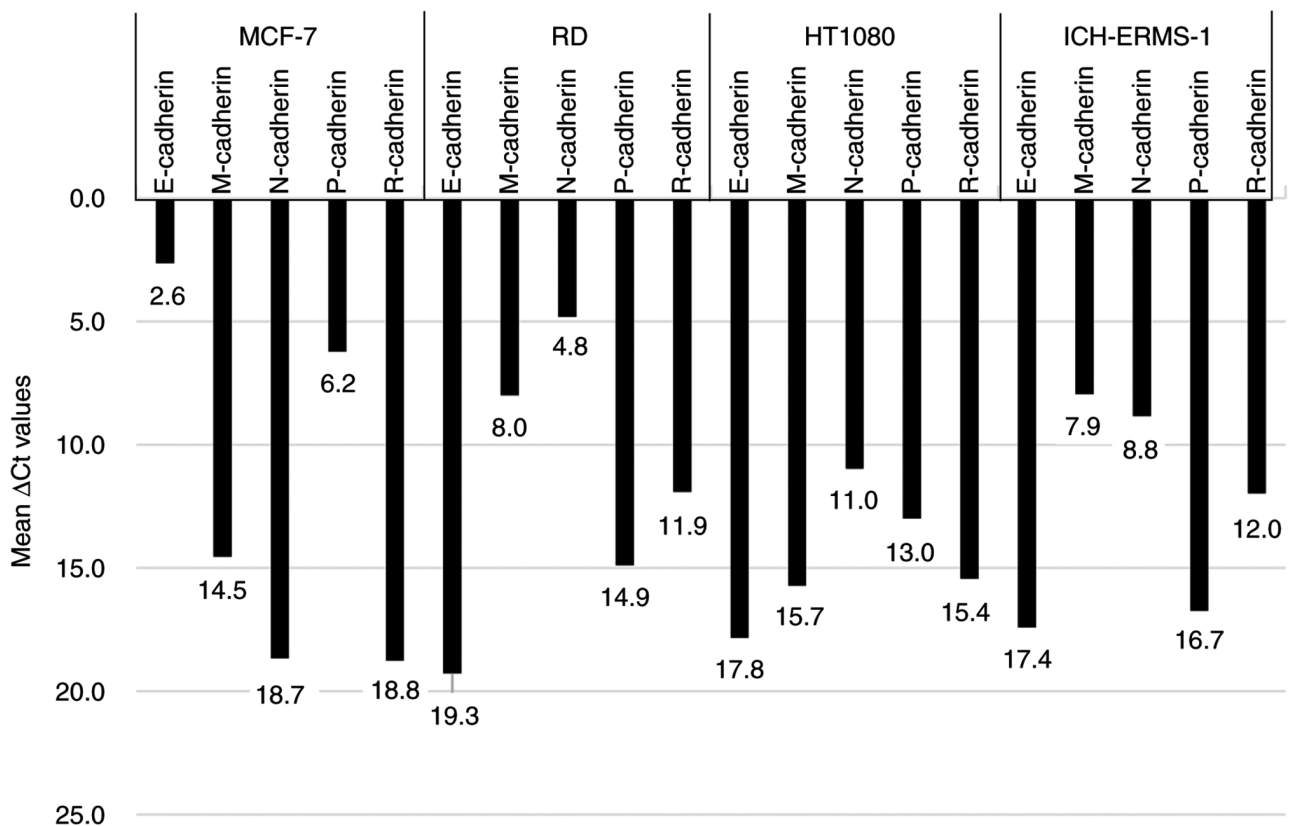


Figure 4. mRNA expression levels of the different members of the cadherin family of genes in the indicated cell lines. Data are presented as mean ΔC_t values, and GAPDH was used as the reference gene. A small ΔC_t value indicates a higher mRNA expression level.

entosis (1). Sun *et al* (17) reported that the introduction of E- or P-cadherin in cadherin-negative breast cancer cell lines induced entosis, demonstrating the role of cadherin proteins in entosis. During entosis, a multimolecular complex termed the mechanical ring is formed in the interface between the cellular surfaces of the invading and host cells; this complex consists of E-cadherin; α -, β -, and γ -catenin; F-actin; vinculin; and other components (2). In the present study, we found that N-cadherin, and not E- or P-cadherin, was involved in the entosis of nonepithelial cells. The cadherin family of proteins includes E-cadherin (33,34), N-cadherin (33), and P-cadherin (35), and N- and E-cadherin fulfill similar roles in cell adhesion (35). Notably, increased N-cadherin expression is observed in some rhabdomyosarcoma cell lines, including the RD cell line (36), although it is not expressed in striated muscle (37). Thus, N-cadherin might function as an adhesion molecule in the entosis of nonepithelial cells.

RD, an embryonal rhabdomyosarcoma cell line, is originally less invasive than alveolar rhabdomyosarcoma cell lines (38). Therefore, the entosis of RD cells cannot be explained as inherently invasive behavior. Instead, the matrix detachment condition might alter their behavior. Li *et al* (39) demonstrated that RD cells cultured under spheroid conditions exhibited enhanced migration compared with those cultured under adherent conditions. In addition, during entosis, the mobility of inner cells increases, and they themselves invade outer cells (17). Our experiments under nonadherent conditions created a situation where cells showed three-dimensional overlapping, which might have altered the mobility of RD cells,

creating conditions favorable for entosis. Thus, in nonepithelial cells, entosis may occur when the environment surrounding tumor cells changes. Because there are no articles specifically mentioning entosis in non-epithelial tumor cells, we would like to speculate on the meanings and significance of entosis in non-epithelial tumor cells by reviewing the phenomenon as reported in epithelial tumor cells. What should be understood from reports on the incidence of CIC and the prognosis of cancer patients is that the relationship between CIC incidence and prognosis varies depending on the type of cancer. For example, Schwegler *et al* (40) found that lower incidences of CIC in head and neck cancer and colorectal cancer were associated with a better patient prognosis, while a higher incidence of CIC in anal cancer was associated with a better patient prognosis. Song *et al* (10) reported that the prognosis of pancreatic cancer patients was worse in cases where CIC was observed. In addition, Druzhkova *et al* (41) showed that the incidence of CIC in colon cancer cell lines increased depending on the chemotherapy drug concentration. In other words, considering the above reports, regarding whether the appearance of CIC has a pro-tumor or anti-tumor effect, it appears that the majority of reports suggest that CIC formation has a pro-tumor effect. Therefore, even in non-epithelial tumors, the significance of CIC formation may be understood more in terms of its possible role as a poor prognostic factor or as a means of escaping from anticancer drugs, rather than its anti-tumor effect. Further studies are needed to confirm this implication.

Homotypic CIC structures can also occur in cannibalism, which, however, usually arises under starvation

conditions (14). Additionally, other molecules, such as ezrin, actin, and caveolin-1, play roles in cannibalism but not in entosis (11,42). Therefore, the accumulating data suggests that the CIC observed in the present study is not an indication of cannibalism.

We acknowledge the limitations of the present study. Among the three nonepithelial cell lines analyzed in the present study, entosis was observed only in RD cells. Thus, experiments utilizing additional nonepithelial cell lines are necessary to confirm our study findings. Additionally, we examined only the role of N-cadherin in nonepithelial cell-related entosis and did not expand our evaluations to other potential molecules. Furthermore, we did not evaluate the histologic aspects of nonepithelial cell entosis due to the lack of clinical samples containing rhabdomyosarcoma cells collected from body cavities.

In conclusion, this is the first study to demonstrate that entosis, a phenomenon previously considered to be limited to epithelial cells, could occur in nonepithelial cells. We also show that nonepithelial cell entosis involves N-cadherin, but not E-cadherin, an entotic finding not previously reported.

Acknowledgements

Not applicable.

Funding

No funding was received.

Availability of data and materials

The data generated in the present study may be requested from the corresponding author.

Authors' contributions

MO performed cell-in-cell (CIC) structure-related culture experiments, developed the cell block preparation technique and prepared cell blocks, manually counted CIC structures and counted total cells by computer-assisted image analysis, performed RNA extraction, cDNA preparation and quantitative PCR analysis, prepared figures and tables, and wrote all parts of the draft of this manuscript. MS conducted the research as the principal investigator, cultured and maintained the cell lines, supervised cell culture, RNA extraction and cDNA preparation, evaluated the CIC structures, reviewed the data, figures and tables, reviewed all contents of the manuscript written by MO, and revised all of the descriptions and references as the corresponding author. RK and YK developed the cell block preparation technique and prepared the cell blocks. SK performed RNA extraction, cDNA preparation and quantitative PCR analysis. YN participated in the preparation of cell blocks. MO and MS confirmed the authenticity of all the raw data. All authors have read and approved the final version of the manuscript.

Ethics approval and consent to participate

Not applicable.

Patient consent for publication

Not applicable.

Competing interests

The authors declare that they have no competing interests.

References

- Overholtzer M, Mailleux AA, Mouneimne G, Normand G, Schnitt SJ, King RW, Cibas ES and Brugge JS: A nonapoptotic cell death process, entosis, that occurs by cell-in-cell invasion. *Cell* 131: 966-979, 2007.
- Wang M, Niu Z, Qin H, Ruan B, Zheng Y, Ning X, Gu S, Gao L, Chen Z, Wang X, *et al*: Mechanical ring interfaces between adherens junction and contractile actomyosin to coordinate entotic cell-in-cell formation. *Cell Rep* 32: 108071, 2020.
- Wang M, Ning X, Chen A, Huang H, Ni C, Zhou C, Yu K, Lan S, Wang Q, Li S, *et al*: Impaired formation of homotypic cell-in-cell structures in human tumor cells lacking alpha-catenin expression. *Sci Rep* 5: 12223, 2015.
- Bauer MF, Hildebrand LS, Rosahl MC, Erber R, Schnellhardt S, Büttner-Herold M, Putz F, Ott OJ, Hack CC, Fietkau R and Distel L: Cell-in-cell structures in early breast cancer are prognostically valuable. *Cells* 12: 81, 2022.
- Dziuba I, Gaweł AM, Tyrna P, Machtyl J, Olszanecka M, Pawlik A, Wójcik C, Biały LP and Młynarczyk-Biały I: Homotypic entosis as a potential novel diagnostic marker in breast cancer. *Int J Mol Sci* 24: 6819, 2023.
- Wei Y, Niu Z, Hou X, Liu M, Wang Y, Zhou Y, Wang C, Ma Q, Zhu Y, Gao X, *et al*: Subtype-based analysis of cell-in-cell structures in non-small cell lung cancer. *Am J Cancer Res* 13: 1091-1102, 2023.
- Liu X, Guo R, Li D, Wang Y, Ning J, Yang S and Yang J: Homotypic cell-in-cell structure as a novel prognostic predictor in non-small cell lung cancer and frequently localized at the invasive front. *Sci Rep* 14: 18952, 2024.
- Almangush A, Mäkitie AA, Hagström J, Haglund C, Kowalski LP, Nieminen P, Coletta RD, Salo T and Leivo I: Cell-in-cell phenomenon associates with aggressive characteristics and cancer-related mortality in early oral tongue cancer. *BMC Cancer* 20: 843, 2020.
- Kim Y, Choi JW, Lee JH and Kim YS: Spindle assembly checkpoint MAD2 and CDC20 overexpressions and cell-in-cell formation in gastric cancer and its precursor lesions. *Hum Pathol* 85: 174-183, 2019.
- Song J, Xu R, Zhang H, Xue X, Ruze R, Chen Y, Yin X, Wang C and Zhao Y: Cell-in-cell-mediated entosis reveals a progressive mechanism in pancreatic cancer. *Gastroenterology* 165: 1505-1521.e20, 2023.
- Lugini L, Matarrese P, Tinari A, Lozupone F, Federici C, Iessi E, Gentile M, Luciani F, Parmiani G, Rivoltini L, *et al*: Cannibalism of live lymphocytes by human metastatic but not primary melanoma cells. *Cancer Res* 66: 3629-3638, 2006.
- Gupta K and Dey P: Cell cannibalism: Diagnostic marker of malignancy. *Diagn Cytopathol* 28: 86-87, 2003.
- Wang S, He M, Li L, Liang Z, Zou Z and Tao A: Cell-in-cell death is not restricted by caspase-3 deficiency in MCF-7 cells. *J Breast Cancer* 19: 231-241, 2016.
- Fais S: Cannibalism: A way to feed on metastatic tumors. *Cancer Lett* 258: 155-164, 2007.
- Humble JG, Jayne WH and Pulvertaft RJ: Biological interaction between lymphocytes and other cells. *Br J Haematol* 2: 283-294, 1956.
- Larsen TE: Emperipolesis of granular leukocytes within megakaryocytes in human hemopoietic bone marrow. *Am J Clin Pathol* 53: 485-489, 1970.
- Sun Q, Cibas ES, Huang H, Hodgson L and Overholtzer M: Induction of entosis by epithelial cadherin expression. *Cell Res* 24: 1288-1298, 2014.
- Sun Q, Luo T, Ren Y, Florey O, Shirasawa S, Sasazuki T, Robinson DN and Overholtzer M: Competition between human cells by entosis. *Cell Res* 24: 1299-1310, 2014.
- Kianfar M, Balcerak A, Chmielarczyk M, Tarnowski L and Grzybowska EA: Cell death by entosis: Triggers, molecular mechanisms and clinical significance. *Int J Mol Sci* 23: 4985, 2022.

20. Krajcovic M, Johnson NB, Sun Q, Normand G, Hoover N, Yao E, Richardson AL, King RW, Cibas ES, Schnitt SJ, *et al*: A non-genetic route to aneuploidy in human cancers. *Nat Cell Biol* 13: 324-330, 2011.
21. Liang J, Niu Z, Zhang B, Yu X, Zheng Y, Wang C, Ren H, Wang M, Ruan B, Qin H, *et al*: p53-dependent elimination of aneuploid mitotic offspring by entosis. *Cell Death Differ* 28: 799-813, 2021.
22. Wen S, Shang Z, Zhu S, Chang C and Niu Y: Androgen receptor enhances entosis, a non-apoptotic cell death, through modulation of Rho/ROCK pathway in prostate cancer cells. *Prostate* 73: 1306-1315, 2013.
23. Zhang X, Niu Z, Qin H, Fan J, Wang M, Zhang B, Zheng Y, Gao L, Chen Z, Tai Y, *et al*: Subtype-based prognostic analysis of cell-in-cell structures in early breast cancer. *Front Oncol* 9: 895, 2019.
24. Ishikawa F, Ushida K, Mori K and Shibamura M: Loss of anchorage primarily induces non-apoptotic cell death in a human mammary epithelial cell line under atypical focal adhesion kinase signaling. *Cell Death Dis* 6: e1619, 2015.
25. Wang C, Chen A, Ruan B, Niu Z, Su Y, Qin H, Zheng Y, Zhang B, Gao L, Chen Z, Tai Y, *et al*: PCDH7 inhibits the formation of homotypic cell-in-cell structure. *Front Cell Dev Biol* 8: 329, 2020.
26. Durgan J, Tseng YY, Hamann JC, Domart MC, Collinson L, Hall A, Overholtzer M and Florey O: Mitosis can drive cell cannibalism through entosis. *Elife* 6: e27134, 2017.
27. Mackay HL, Moore D, Hall C, Birkbak NJ, Jamal-Hanjani M, Karim SA, Phatak VM, Piñon L, Morton JP, Swanton C, *et al*: Genomic instability in mutant p53 cancer cells upon entotic engulfment. *Nat Commun* 9: 3070, 2018.
28. Bozkurt E, Dussmann H, Salvucci M, Cavanagh BL, Van Schaeybroeck S, Longley DB, Martin SJ and Prehn JHM: TRAIL signaling promotes entosis in colorectal cancer. *J Cell Biol* 220: e202010030, 2021.
29. Garanina AS, Kisurina-Evgenieva OP, Erokhina MV, Smirnova EA, Factor VM and Onishchenko GE: Consecutive entosis stages in human substrate-dependent cultured cells. *Sci Rep* 7: 12555, 2017.
30. Rao X, Huang X, Zhou Z and Lin X: An improvement of the 2^{-(delta delta CT)} method for quantitative real-time polymerase chain reaction data analysis. *Biostat Bioinforma Biomath* 3: 71-85, 2013.
31. Uehata M, Ishizaki T, Satoh H, Ono T, Kawahara T, Morishita T, Tamakawa H, Yamagami K, Inui J, Maekawa M and Narumiya S: Calcium sensitization of smooth muscle mediated by a Rho-associated protein kinase in hypertension. *Nature* 389: 990-994, 1997.
32. Gutjahr MC, Rossy J and Niggli V: Role of Rho, Rac, and Rho-kinase in phosphorylation of myosin light chain, development of polarity, and spontaneous migration of Walker 256 carcinosarcoma cells. *Exp Cell Res* 308: 422-438, 2005.
33. Hatta K, Okada TS and Takeichi M: A monoclonal-antibody disrupting calcium-dependent cell cell-adhesion of brain-tissues-possible role of its target antigen in animal pattern-formation. *Proc Natl Acad Sci USA* 82: 2789-2793, 1985.
34. Yoshida-Noro C, Suzuki N and Takeichi M: Molecular nature of the calcium-dependent cell cell-adhesion system in mouse teratocarcinoma and embryonic-cells studied with a monoclonal-antibody. *Dev Biol* 101: 19-27, 1984.
35. Nose A and Takeichi M: A novel cadherin cell-adhesion molecule: Its expression patterns associated with implantation and organogenesis of mouse embryos. *J Cell Biol* 103 (6 Pt 2): 2649-2658, 1986.
36. Soler AP, Johnson KR, Wheelock MJ and Knudsen KA: Rhabdomyosarcoma-derived cell-lines exhibit aberrant expression of the cell-cell adhesion molecules N-Cadherin, and cadherin-associated proteins. *Exp Cell Res* 208: 84-93, 1993.
37. Derycke LD and Bracke ME: N-cadherin in the spotlight of cell-cell adhesion, differentiation, embryogenesis, invasion and signalling. *Int J Dev Biol* 48: 463-476, 2004.
38. Rapa E, Hill SK, Morten KJ, Potter M and Mitchell C: The over-expression of cell migratory genes in alveolar rhabdomyosarcoma could contribute to metastatic spread. *Clin Exp Metastasis* 29: 419-429, 2012.
39. Li M, Nagamori E and Kino-Oka M: Disruption of myoblast alignment by highly motile rhabdomyosarcoma cell in tissue structure. *J Biosci Bioeng* 123: 259-264, 2017.
40. Schwegler M, Wirsing AM, Schenker HM, Ott L, Ries JM, Büttner-Herold M, Fietkau R, Putz F and Distel LV: Prognostic value of homotypic cell internalization by nonprofessional phagocytic cancer cells. *Biomed Res Int* 2015: 359392, 2015.
41. Druzhkova I, Potapov A, Ignatova N, Bugrova M, Shchepochkin I, Lukina M, Shimolina L, Kolesnikova E, Shirmanova M and Zagaynova E: Cell hiding in colorectal cancer: Correlation with response to chemotherapy in vitro and in vivo. *Sci Rep* 14: 28762, 2024.
42. Lugini L, Lozupone F, Matarrese P, Funaro C, Luciani F, Malorni W, Rivoltini L, Castelli C, Tinari A, Piris A, *et al*: Potent phagocytic activity discriminates metastatic and primary human malignant melanomas: A key role of ezrin. *Lab Invest* 83: 1555-1567, 2003.



Copyright © 2025 Oi et al. This work is licensed under a Creative Commons Attribution-NonCommercial-NoDerivatives 4.0 International (CC BY-NC-ND 4.0) License.